

# Development of an Experimental Facility for Impact Testing of Armour Plates

M. Raguraman<sup>1,†,\*</sup>, G. Jagadeesh<sup>2</sup> and A. Deb<sup>3</sup>

<sup>1</sup>School of Mechanical Engineering, University of Leeds, UK

<sup>2</sup>Department of Aerospace Engineering, Indian Institute of Science, Bangalore, India

<sup>3</sup>Centre for Product Design and Manufacturing, Indian Institute of Science, Bangalore, India

R.Munusamy@leeds.ac.uk

## Abstract

The present paper deals with the development of a facility for ballistic impact testing of materials for aerospace, automotive and defence applications. In order to validate this setup, experiments have been conducted on commercial grade 1100 aluminium alloy plates of 1 mm thickness with projectiles of four different nose shapes. The impact and residual velocity and the penetration process of all the test cases are recorded using a high-speed video camera. Additionally, with the aid of a general LS-DYNA-based numerical procedure, simulations have been carried out for all the above test cases. The numerical results are found to match well with the experimental observations.

## NOMENCLATURE

$p$	working pressure
$a$	inner radius of tube
$b$	outer radius of tube
$\sigma_y$	yield strength
$N$	factor of safety
1-D	one dimensional

## 1. INTRODUCTION

With the advancement in the availability of computational resources in recent times, numerical codes are increasingly being used as a design tools. Many commercial codes like LS-DYNA are used for designing and analysing the stress levels in armour plates and automobile bumpers. The results from these numerical codes have to be validated with results from careful experiments in ground test facilities. The main aim of this investigation to design and build a projectile launch system that can generate reliable experimental data for validating various numerical codes that are being used by the industry in impact dynamics. Before the study a comprehensive literature survey was carried out to learn about the experimental facilities that have been used for these kinds of studies. The study reveals that the majority of academic projectile impact testing facilities is gas gun type launchers. Gupta et al. [1-3] used a pneumatic gun to launch a projectile with a carrier. The launching device is attached to a long barrel with a stopper at the exit end for intercepting the carrier just before the projectile leaves the barrel. Infrared emitters with a matching number of photodiodes on either side of projectile path are fixed at known distances ahead of the target plate to measure the time of flight from which the impact velocity is deduced. For measuring residual velocity, two sets of aluminium foil screens have been used which are successively pierced by a projectile as it emerges after perforating the target plate.

Borvik et al. [4-7] used a compressed gas gun to launch projectiles. The main components are a pressure tank with a capacity of 200 bar, a firing unit, a 10 m long smooth barrel, and a closed impact chamber. The gas gun was designed to launch a projectile with a mass of 250 grams to a maximum velocity of 1000 m/s when helium was used as the propellant. A gas gun facility was also used for propelling projectiles by Billion and Robinson [8]. They used nitrogen or helium as the propelling gas.

\*Corresponding author: r.munusamy@leeds.ac.uk; Telefax: +44 113 242 4611

†Formerly with the Centre for Product design and Manufacturing, Indian Institute of Science, Bangalore, India.

The gun was designed to propel projectiles of either 5.59 mm or 7.62 mm diameter at velocities in the range of 200-750 m/s. In order to achieve impact velocities at the higher end of ordnance range, Gupta and Madhu [9] used rifle gun for firing projectiles. The test facility consisted of a firing chamber, a long barrel and an observation chamber. The target-holding fixture was located at a distance of 10 m from the gun. The impact and residual velocities of the projectile were measured in the tests using four aluminium foil screens. The first two screens were used for measuring initial velocity of projectile and the remaining two for the residual velocity.

With the consideration of the weaknesses of the existing setups [1-9], a test apparatus has been developed for impact testing of plates and the features of the same is reported in this paper. The details of the impact tests carried out using the developed facility on grade 1100 aluminium alloy plates of 1 mm thickness with four different nose-shaped projectiles are also reported in this paper. Finally, using a general LS-DYNA-based simulation procedure, the computed residual velocity is compared with the corresponding test residual velocity and the target plate failure pattern is examined for all the test cases.

## 2. DEVELOPMENT OF A BALLISTIC IMPACT TESTING APPARATUS

Existing impact testing facilities reported in the literature have been studied and based on this the initial design specification of the device was assumed. The length of the launch tube which is a critical component of the device has been determined using a one-dimensional Lagrangian code. The wall thickness of all the components was computed based on maximum shear stress theory. Using these dimensions, a CAD model was generated and the apparatus was fabricated. The development process is detailed in the following sub-sections.

### 2.1. Concept and requirements

A schematic diagram of the facility is shown in Figure 1. The facility consists of three major components, viz. a pressure chamber, a launch tube and a test chamber. A piston is placed in the pressure chamber and is drawn inwards by vacuum by opening the control valve CV1 connected to a vacuum pump. High pressure is created in the pressure chamber by opening the control valve CV2 connected to a cylinder containing compressed nitrogen. The pressure in the chamber is adjusted depending upon the velocity with which the projectile has to hit the target. The control valves CV1 and CV2 are then closed, and the vacuum pump switched off. On opening the control valve CV3, the carrier (also called as piston or sabot) will be accelerated through the launch tube. The stopper is fixed at the other end of launch tube which stops the piston and helps to eject the projectile. The target plate is fixed inside the test chamber. The projectile either perforates or ricochets off the target after hitting it but stays inside the test chamber, thereby posing minimum risk to the laboratory personnel. The requirements of the current apparatus are as follows: (i) The maximum velocity to be attained is 200 m/s, and (ii) the maximum mass to be accelerated is 100 grams of projectile mass or the carrier mass of up to 1 kg.

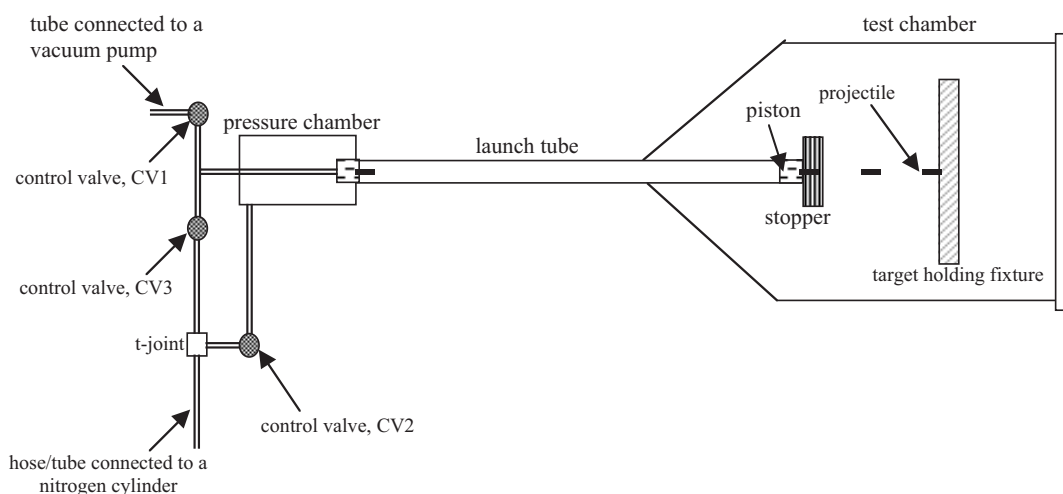


Figure 1. Schematic diagram of proposed experimental setup

## 2.2. Determination of initial dimensions using 1-D Lagrangian code

The one-dimensional Lagrangian code is developed to model the quasi-one-dimensional gas-dynamic processes within transient-flow facilities [10]. The class of facilities that can be modelled includes free-piston shock tunnels, expansion tubes and light-gas guns. The simulation can include multiple (interacting) gas slugs, pistons and diaphragms but the primary flow interactions have to be along the axis of the facility. The numerical modelling is based on a quasi-one-dimensional, Lagrangian description of the gas dynamics coupled with engineering correlations for viscous effects and point-mass dynamics for piston motion. This essentially means that the code tracks a number of fixed masses of gas (and pistons) as they travel along a tube of varying area. A simulation can include slugs of gas (consisting of a large number of fixed-mass gas cells) pushing on, or being pushed by, a number of pistons. As in real facilities, the interactions between gas slugs can be controlled by the inclusion of diaphragms which can be set to rupture when specified pressure differences are exceeded [10].

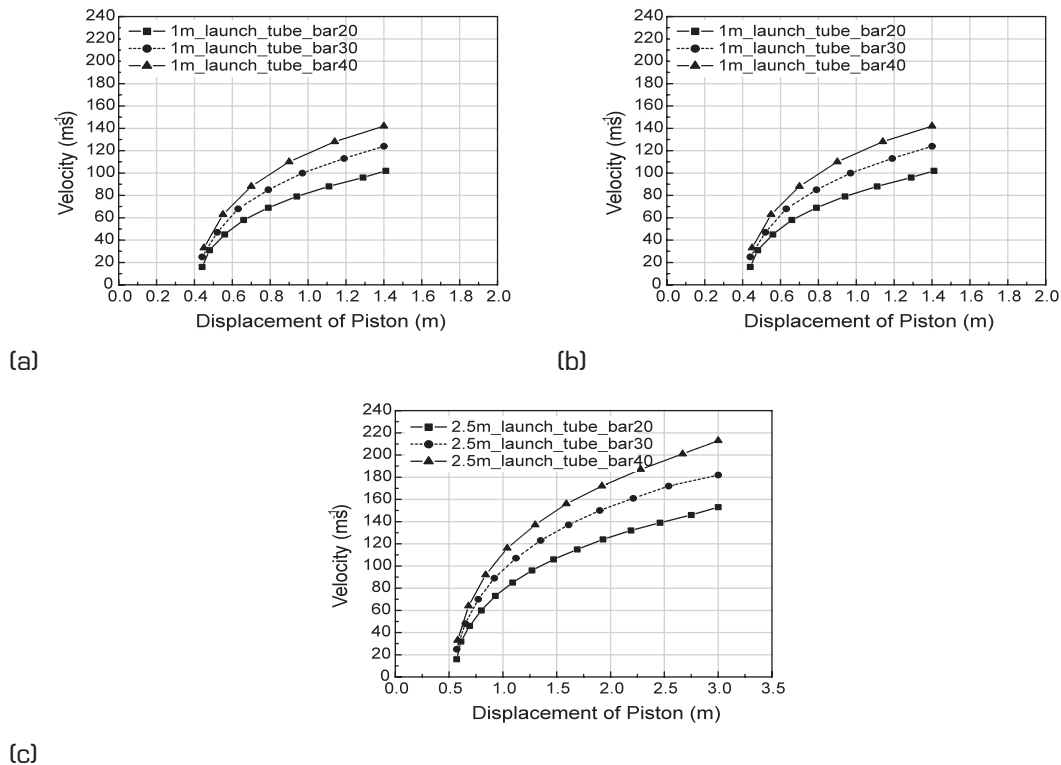


Figure 2. Velocity profiles when piston moves in a tube of (a) 1m length, (b) 2 m length and (c) 2.5 m length

Parameters such as mass of piston = 1 kg, diameter of piston = 75 mm, length of piston = 200 mm, material of piston = nylon (density =  $1100 \text{ kg m}^{-3}$ ), diameter of pressure chamber = 240 mm, length of pressure chamber = 400 mm, diameter of test chamber = 600 mm, and length of test chamber = 2000 mm were considered as input data. The launch tube length was varied until the maximum impact velocity of  $\sim 200 \text{ m/s}$  was obtained. It may be noted that the assumed material for pressure chamber, test chamber and launch tube was mild steel. The velocity versus displacement profile of piston obtained through 1-D Lagrangian code simulations for different cases are shown in Figure 2. The percentage variation of velocity for a given tube length is approximately the same for every 10 bar pressure increment. This indicated that the velocity increases only with increase in the length of launch tube for a given pressure input. Hence, any length of mild steel tube can be chosen when nylon piston is used because the friction between these two materials is almost negligible. The length of 2 m was selected in the present case because it met the maximum velocity of 200 m/s for a maximum pressure input of 40 bar.

### 2.3. Detailing of wall thicknesses of components

Wall thicknesses of pressure chamber and launch tube were calculated using the relation given in (1) from [11] based on maximum shear stress theory;

$$p \frac{(b^2 + a^2)}{(b^2 - a^2)} = \frac{\sigma_y}{N} \quad (1)$$

where,  $p$  is a working pressure,  $a$  is inner radius of tube,  $b$  is outer radius of tube,  $\sigma_y$  is the yield strength and  $N$  is the safety factor. The wall thicknesses of the pressure chamber and the launch tube were estimated using Equation (1) and validated through plane strain finite element analysis using ANSYS 10.0. The wall thickness of the annular plate connecting the pressure chamber to the launch tube was estimated by carrying out a transverse bending analysis using shell elements. The maximum von Mises stress obtained for various wall thicknesses along with the computed factors of safety are listed in Table 1, based on which the wall thicknesses were finalized. The selected thickness of various components is highlighted in bold in Table 1.

**Table 1. Maximum Von Mises stress obtained through simulation**

Components	Wall thickness (mm)	Maximum Von Mises stress (MPa) obtained ANSYS-based simulation	Factor of safety, N
Pressure chamber	10.0	87.87	2.3
	<b>25.0</b>	<b>27.20</b>	<b>7.4</b>
Launch tube	5.0	63.04	3.2
	<b>10.0</b>	<b>36.50</b>	<b>5.5</b>
Connecting plate between pressure chamber and launch tube	10.0	317.63	0.6
	<b>25.0</b>	<b>55.99</b>	<b>3.6</b>

A CAD model was then generated and detailed drawings of individual components of the above apparatus were prepared. Based on the drawings, the components were machined maintaining the required accuracy especially in the launch tube inner surface. The final assembled test setup is shown in Figure 3. In the present setup, a slot with a transparent screen is provided in the test chamber for carrying out a digital video recording of the impact event with an externally placed high-speed camera. This procedure yielded complete information on the path of projectile before and after impact, angle of obliquity, and initial as well as residual velocities.

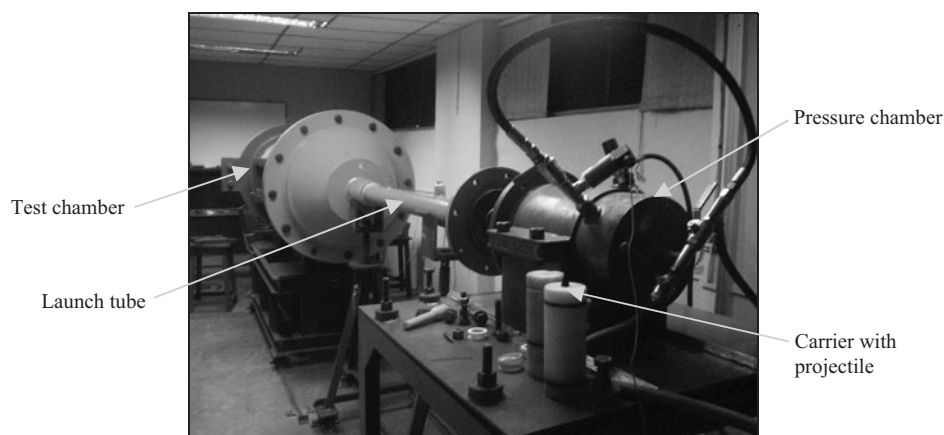


Figure 3. Ballistic impact testing apparatus in Product Safety Laboratory, CPDM, IISc

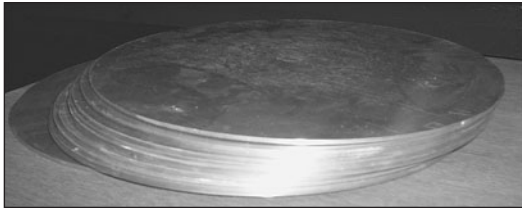
### 2.4. Problems associated with the facility during the development

During an impact event, the total impact force will act on the stopper which is fixed at the other end of launch tube from where projectile ejects. The stopper was made initially of mild steel and the impact face is covered with nylon which is same as the piston material. The stopper was crushed and broken

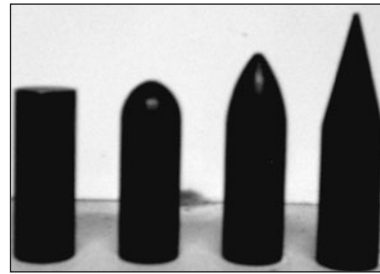
into bits and pieces after a few impacts which indicated that there is a need for selecting material with high strength and energy absorbing capacity. Hence, the stopper is now manufactured with stainless steel and the impact face is shielded with polypropylene.

### 3. IMPACT TESTING OF THIN ALUMINIUM PLATES

Commercially available 1 mm thick Al 1100 aluminium plates were cut into circular pieces with a diameter of 255 mm followed by trimming of edges. Projectiles of different nose shapes such as conical, ogival, hemispherical and blunt with a diameter of 15 mm were machined from steel rods by turning and subsequently hardened to a hardness range of 50-52  $R_c$ . Each finished projectile weighed  $55 \pm 0.1$  grams. Target plates and projectiles are shown in their final form in Figures 4 (a) and (b) respectively.



(a)



(b)

Figure 4. Finished form of: (a) target plates and (b) projectiles

A target plate was rigidly fixed in a fixture with a free span of 205 mm diameter as shown in Figure 5. The projectile was placed in a carrier (also called as sabot or piston) as shown in Figure 6. The whole set was then inserted into the pressure chamber as shown in Figure 7. The pressure chamber and launch tube were then connected rigidly with a number of bolts as shown in Figure 8 and the vacuum pump was turned on. The pressure chamber was now filled to the required pressure by opening a valve connected to a nitrogen gas cylinder; finally the vacuum pump was turned off and the projectile was launched. A Phantom 7.2 high-speed camera (Ms. Vision Research USA) was activated just prior to the projectile launch and the impact event was recorded.



(a) Component fixture with target plate



(b) Fixture with plate inside the test chamber

Figure 5. Target plate holding fixture

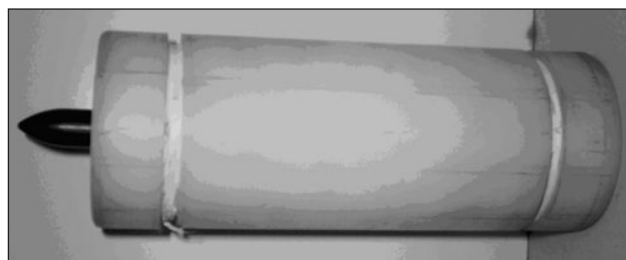


Figure 6. Projectile placed in a carrier

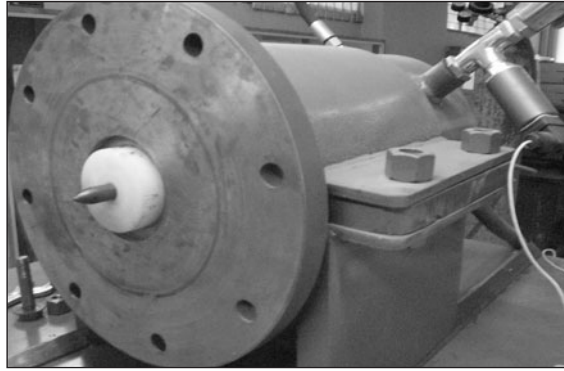


Figure 7. Projectile with carrier placed inside the pressure chamber

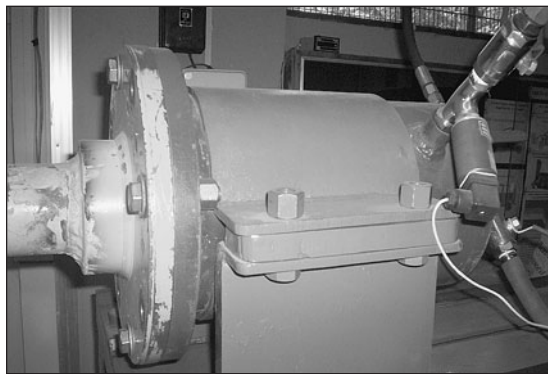


Figure 8. Pressure chamber and launch tube connected together

#### 4. RECORDING OF IMPACT EVENT USING A HIGH-SPEED CAMERA

In most of the academic-type testing facilities, aluminium foil screens were used to record incident and residual velocities. Using this technique, it would be difficult to capture the entire impact event or process. However, the high-speed camera can be able to record both impact process and velocities. Hence, a Phantom 7.2 high-speed camera (Ms. Vision Research, USA) that is capable of recording 6688 frames per second at full resolution of 800 x 600 pixel using SR-CMOS imaging array was used in the current experiments. In the present experiments, the stages of the projectile penetration process were recorded by operating the camera at 2000 frames per second with a resolution of 450 x 450 pixels. A 300 W North Star lamp with C-clamp base was used as the continuous light source. Operation of the camera was synchronized with the expected projectile trajectory. The light source was switched on before firing the projectile, and the camera was triggered to synchronize with the projectile launching.

Impact testing was carried out for the four different nose shapes. The computed resultant impact and residual velocities of all the projectiles are listed in Table 2. In the present case, the velocity is measured by considering the displacement of the projectile nose divided by the time taken between two successive frames of the high-speed camera record. The recorded images at various instants of time for the grade 1100 aluminium plates impacted by conical, ogival, hemispherical and blunt nosed projectiles are shown in Figure 9.

**Table 2. Recorded impact and residual velocities of projectiles for various test cases**

Projectile nose shape	Plate thickness (mm)	Impact velocity (m/s)	Angle of impact (degrees)	Recorded resultant residual velocity (m/s)
Conical	1.0	32.04	5.70	25.70
Ogival	1.0	30.70	15.89	24.10
Hemispherical	1.0	33.87	14.49	25.73
Blunt	1.0	34.79	4.80	23.10

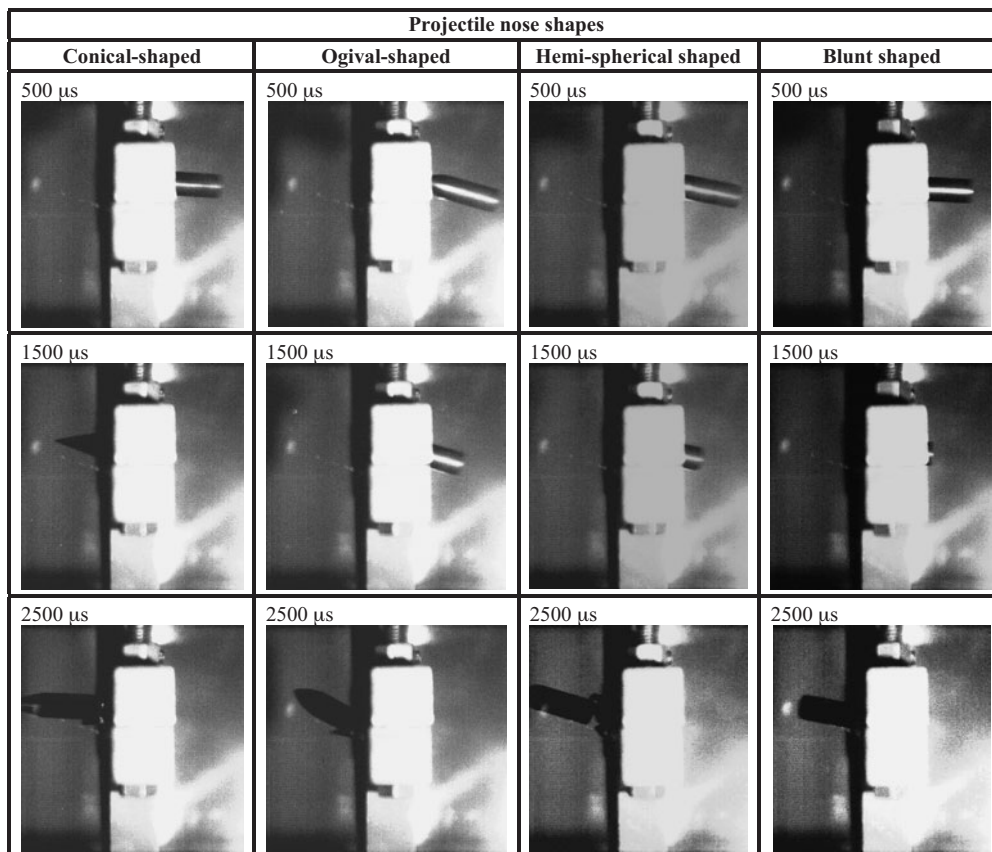


Figure 9. Recorded images of projectile penetration process using a high speed camera

## 5. VALIDATION OF MEASURED VELOCITIES USING 1-D LAGRANGIAN CODE

After fabrication, the dimensions of all components were measured. Using these dimensions, once again simulation was carried out with the 1-D Lagrangian code in order to validate the tested and simulation-based results. Projectile impact velocity of 29.82 m/s was obtained in the current simulation which matches well with the test-based impact velocity for all the test cases shown in the column 3 of Table 2 which indicated the reliability of current approach of designing a new type of impact testing facility.

## 6. NUMERICAL VALIDATION USING LS-DYNA

A finite element modelling procedure for analysing projectile impact on thin aluminium plates described in [12, 13] was used for simulating the current test cases using LS-DYNA. The finite element models of target plate and projectile using Belytschko-Lin-Tsay (BLT) shell elements of 2 mm size and solid elements respectively are shown in Figure 10. The shape and size of the target plate and projectile and the impact conditions considered for modelling were the same as the test cases defined in Table 1. The Contact\_Eroding\_Surface\_Surface (CESS) interface was defined between target plate and projectile.

A strain-rate dependent plasticity model (material type 19 in LS-DYNA) was used for defining the behaviour of the target aluminium plate. The true stress versus true strain behaviour of the target material required for this material model was described in [12, 13]. The projectile was modelled with material type 24 used in LS-DYNA for defining piecewise linear elasto-plastic behaviour. The hardness of the projectile material specified in Section 3 (i.e. 50-52  $R_c$ ) was found to be comparable to that of AISI A2 tool steel at a hardening temperature of 595-C as given in [15]. Hence the properties of this hardened steel were chosen for defining the projectile material in the current simulations. For all analyses carried out here, the visco-plastic formulation option was used for both plate and projectile materials.

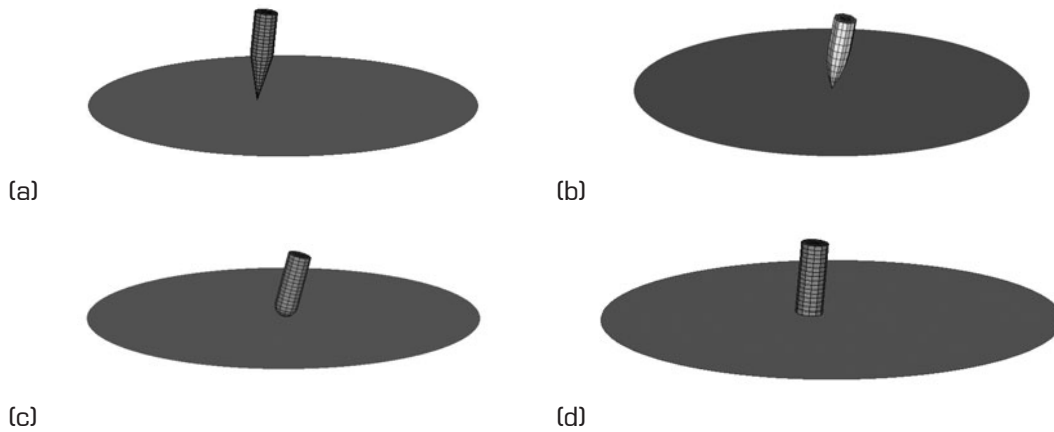


Figure 10. Finite element models of circular target plates with slightly oblique (a) conical-head, (b) ogival-head, (c) hemispherical-head, and (d) blunt-head projectiles (before impact)

Simulations have been carried out for the four test cases corresponding to the four different shaped projectiles shown in Figure 4(b). The impact velocities measured in the four tests considered are given in Table 1 and each of these was the specified projectile initial velocity in the simulation. The angle of obliquity of impact was also specified by rotating the projectile from its normal axis according to the measured values of the angles given in column 4 of Table 1. The resultant residual velocity predicted in each case through analysis is compared with the test-based residual velocity in Table 3 and a good correlation is seen with a maximum deviation between computed and observed residual velocities of only 4.3%. It may be noted that the use of the high-speed camera made possible a very accurate assessment of the initial angle of obliquity as well as the resultant residual velocity in the direction of motion of the projectile after plate perforation.

**Table 3. Comparison of projectile residual velocity for different nose shapes**

Projectile nose shape	Plate thickness (mm)	Impact velocity (m/s)	Angle of obliquity (degrees)	Resultant residual velocity (m/s)		% deviation from test
				Test	Simulation	
Conical	1.0	32.0	5.7	25.7	25.1	-2.3
Ogival	1.0	30.7	15.9	24.1	23.8	-1.2
Hemispherical	1.0	33.9	14.5	25.7	24.9	-3.1
Blunt	1.0	34.8	4.8	23.1	22.1	-4.3

The analysis-based snap-shots of plate perforation by projectile are compared in Figures 11 and 12 with the recorded video images at matching times for the four test cases given in Table 2. In the video images, the projectile remains partially hidden in the side view due to obstruction by the frame holding the target plate. However, it appears from the last pair of images in each of these figures that the ejection of the projectile in the simulation matches quite well with the corresponding experimental image of the projectile emerging after plate perforation. Truncated close-up views of actual and simulated plate failures are compared in Table 4. In the first three cases of perforation by conical, ogival, and hemispherical nosed projectiles, plate failure in the tests was associated with petalling but no clear plug formation; similar failure patterns were also obtained through analysis. For the last case of blunt projectile impact, a nearly circular plug was formed which remained thinly attached to the hole boundary; a strikingly similar plug has seen in the simulation perforation.

The good correlation of simulation results of projectile residual velocity and plate failure modes with corresponding test data presented in this section confirm that the present finite element modelling procedure using LS-DYNA is a useful tool for the assessment and design of thin aluminium armour plates subject to near normal impacts.

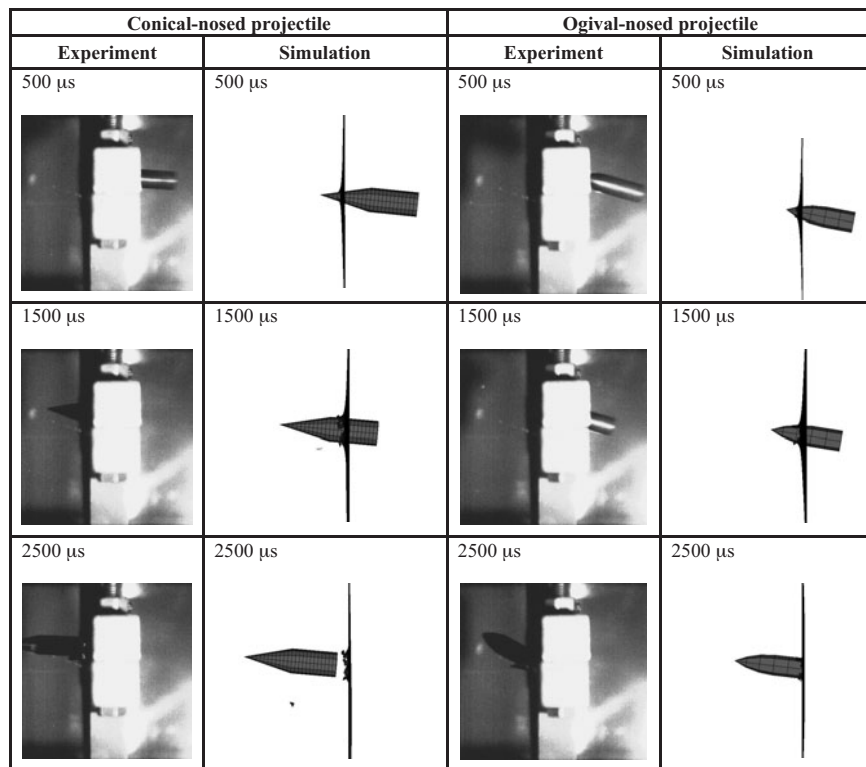


Figure 11. Snap-shots of failure of thin aluminium plate by conical and ogival-nosed projectile impact

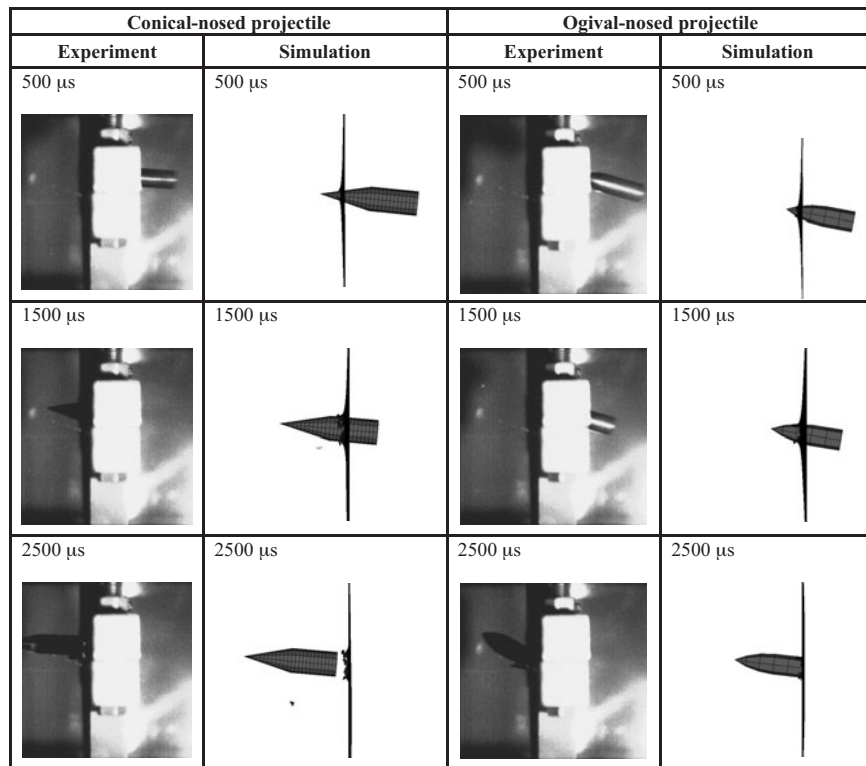
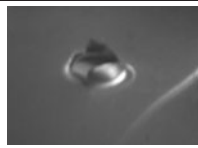
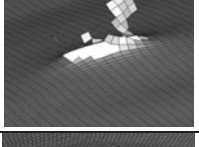
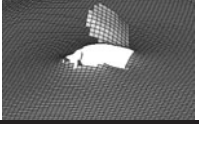


Figure 12. Snap-shots of failure of thin aluminium plate by hemispherical and blunt-nosed projectile impact

**Table 4. Close-up views of actual and simulated plate failures**

Projectile nose shape	Experiment	Simulation
Conical-head		
Ogival-head		
Hemispherical-head		
Blunt-head		

## 6. CONCLUSIONS

In this paper, details of the development of a new gas gun based ballistic impact testing facility were presented. It gives a design guideline to the researchers to build a new type of facility to carry out the experimental studies of projectile impact on aerospace, automotive and defence structures. Usability of the developed set-up and high speed camera for impact on 1 mm thick aluminium plates with projectiles of four different noses is reported. The reliability of obtained results (i.e. impact velocities) using this facility have been verified through L1-D code. Using the developed finite element analysis procedure for aluminium plates with strain rate dependent material behaviour, striking correlation of residual velocity and failure modes with experimental results has been obtained and the same are detailed in this paper. It is concluded that (i) the developed facility can be used with confidence for testing of armour plates, and (ii) the present finite element modelling procedure using LS-DYNA is an excellent tool for the assessment and design of thin aluminium armour plates subject to near normal impacts.

## ACKNOWLEDGEMENTS

The authors would like to thank the Director and Associate Director of IISc for their financial arrangement for the development of present impact testing facility and for importing a high speed camera. We also would like to thank the technical personnel of CPDM workshop and High Enthalpy Laboratory, Aerospace Engineering Department for their help in conducting experiments using this facility.

## REFERENCES

1. Gupta, N.K., Ansari, R. and Gupta, S.K., Normal impact of ogival nosed projectiles on thin plates, *Int. J. Impact Eng*, 2001, 25, 641- 660.
2. Gupta, N.K, Ansari, R. and Gupta, S.K., Normal impact of ogive nosed projectiles on thin plates, *Proc. Implast*, 2003, 711-722.
3. Gupta, N.K, Iqbal, M.A. and Sekhon, G.S., Experimental and numerical studies on the behaviour of thin aluminium plates subjected to impact by blunt- and hemispherical-nosed projectiles, *Int. J. Impact Eng*, 2006, 32(12), 1921-1944.
4. Borvik,T., Langseth, M., Hopperstad, O.S. and Malo, KA., Perforation of 12 mm thick steel plates by 20 mm diameter projectiles with flat, hemispherical and conical noses: Part I: Experimental study, *Int. J. Impact Eng*, 2002, 27, 19 -35.

5. Borvik, T., Hopperstad, O.S., Langseth, M. and Malo, K.A., Effect of target thickness in blunt projectile penetration of Weldox 460 E steel plates, *Int. J. Impact Eng*, 2003, 28, 413 - 464.
6. Borvik, T., Leinum, J.R., Solberg, J.K., Hopperstad, O.S. and Langseth, M., Observations on shear plug formation in Weldox 460 E steel plates impacted by blunt-nosed projectiles, *Int. J. Impact Eng*, 2001, 25, 553 -572.
7. Borvik, T., Langseth, M., Hopperstad, O.S. and Malo, K.A., Ballistic penetration of steel plates, *Int. J. Impact Eng*, 1999, 22, 885 - 886.
8. Billion, H.H. and Robinson, D.J., Models for the ballistic impact of fabric armour, *Int. J. Impact Eng*, 2001, 25, 411- 422.
9. Gupta, N.K. and Madhu, V., An experimental study of normal and oblique impact of hard-core projectile on single and layered plates, *Int. J. Impact Eng*, 1992, 19, 395 - 414.
10. <http://www.mech.uq.edu.au/cfcfd/code/L1d/doc>.
11. Srinath, L.S., Advanced strength of materials, *Tata McGraw-Hill publishing Co*, New Delhi, 1980.
12. Raguraman, M. and Deb, A., Robust prediction of residual velocities and ballistic limits of projectiles for impact on thin aluminium plates, *Proc. SUSI*, 2006, 205 - 206.
13. Raguraman, M., Advanced methodologies for designing metallic armour plates for ballistic impact, PhD Thesis, Indian Institute of Science, 2007.
14. LS-DYNA keyword user's manual version 970, *LSTC*, California, 2003.
15. [www.matweb.com](http://www.matweb.com)

